NASA Technical Memorandum 80085

NASA-TM-80085 19790017893

FULL-SCALE AIRCRAFT SIMULATION WITH CRYOGENIC TUNNELS AND STATUS OF THE NATIONAL TRANSONIC FACILITY

Robert A. Kilgore, William B. Igoe, Jerry B. Adcock, Robert M. Hall, and Charles B. Johnson

April 1979

NASA
National Aeronautics and Space Administration

Langley Research Center
Hampton, Virginia 23665

FULL SCALE AIRCRAFT SIMULATION WITH CRYOGENIC TUNNELS AND STATUS OF THE NATIONAL TRANSONIC FACILITY

R. A. Kilgore, W. B. Igoe, J. B. Adcock,
R. M. Hall, and C. B. Johnson

SUMMARY

Theoretical studies have been made to determine the effect of thermal and caloric imperfections in cryogenic nitrogen on both laminar and turbulent boundary layers. The results indicate that in order to simulate non-adiabatic laminar or turbulent boundary layers in a cryogenic nitrogen wind tunnel, the flight enthalpy ratio, rather than the temperature ratio, should be reproduced. Under adiabatic conditions the difference between wind tunnel and flight boundary layer parameters is negligible except for the surface temperature ratio. No significance can be attached to the difference in temperature ratio. The absence of significant real-gas effects on both viscous and inviscid flows makes it unlikely that there will be large real-gas effects on the cryogenic tunnel simulation of shock boundary-layer interactions or other complex flow conditions encountered in flight.

Experimental and theoretical studies on condensation effects have been made to determine the minimum usable stagnation temperature. Considerable evidence indicates that under most circumstances free-stream Mach number rather than maximum local Mach number determines the relevant saturation boundary and thereby determines the onset of condensation effects. Under extremely high local Mach number conditions, however, homogeneous nucleation could occur and the onset of condensation effects might be seen at temperatures higher than free-stream saturation temperature but still considerably lower than local Mach number saturation temperature.

Progress is well underway on a major application of the cryogenic wind-tunnel concept with the construction of the U.S. National Transonic Facility at the Langley Research Center. This new tunnel is scheduled to become operational by 1982. Not only will it provide an order of magnitude increase in Reynolds number capability over existing U.S. tunnels, but also, because of the ability to vary pressure, Mach number, and temperature independently, it will be able to perform the highly desirable research task of separating aeroelastic, compressibility, and viscous effects on the aerodynamic parameters being measured.

SYMBOLS

a	speed of sound	C_p	pressure coefficient
c	airfoil chord	C_f	local skin-friction coefficient
$\bar{c}$	mean geometric chord	h	specific enthalpy
c_p	specific heat at constant pressure	M	Mach number

p	pressure
q	dynamic pressure
R	Reynolds number
$\mathcal{R}$	gas constant
T	temperature
u	velocity
v	specific volume
x	streamwise coordinate
y	coordinate normal to plate
δ	boundary-layer thickness
δ^*	displacement thickness
θ	momentum thickness
μ	viscosity
ρ	density

Subscripts

aw	adiabatic wall
L	local
max	maximum
min	minimum
t	stagnation conditions
w	wall
∞	free-stream conditions

INTRODUCTION

During the last 10 years or so there has been an ever increasing level of activity devoted to finding a solution to the problem of inadequate test Reynolds number in the existing transonic wind tunnels. The need for increased test Reynolds number and details of many of the schemes proposed to meet the need are documented in papers presented at the AGARD fluid dynamics panel specialists' meetings held in Göttingen[1] in 1971 and in London[2] in 1975. Of the proposed solutions, the cryogenic wind tunnel concept appears to be best in terms of capital and operating costs while offering some unique advantages in research versatility.[3]

The idea of increasing the test Reynolds number and reducing fan power by using a heavy gas or by cooling the gas appears to have been first proposed in 1920 by Margoulis.[4,5] Margoulis correctly concluded that the benefits of moderate cooling were not worth the effort. His idea of cooling the test gas was rather widely known at the time but apparently was dismissed as impractical and forgotten. Some 25 years later, in 1945, a theoretical study by Smelt[6] noted the advantages of using gases other than air and of cooling the test gas to cryogenic temperatures. The lack of a practical means of cooling a tunnel of any appreciable size to cryogenic temperatures precluded application of the cryogenic wind tunnel concept at the time of Smelt's work.

In the autumn of 1971, Goodyer[7], who was working at NASA-Langley at the time, suggested, independently, the use of either air or nitrogen at cryogenic test temperatures as a way of increasing the test Reynolds number in the small tunnels equipped with magnetic-suspension and balance systems. By 1971, the availability of liquified gases in large quantities and the widespread application of cryogenic technology in government and industry made Goodyer's proposal seem reasonable not only for tunnels of modest size but also for large tunnels that would be capable of testing models at full-scale values of Reynolds number.

An additional advantage of a cryogenic wind tunnel is offered by the ability to vary temperature independently of the usual variables of pressure and Mach number. This makes possible the isolation of viscous, aeroelastic, and Mach number effects on the aerodynamic parameters using a single wind tunnel model. Also, by using the appropriate combinations of pressure and temperature, it should be possible to match more accurately the expected full-scale wing deformations while at the same time matching the full-scale values of Reynolds number. In the final analysis, the additional testing versatility offered by having temperature as a variable may be as valuable to the researcher as the ability to achieve full-scale values of Reynolds number.

In order to verify the cryogenic wind tunnel concept, a small fan-driven closed-circuit low-speed atmospheric tunnel at Langley was modified

for cryogenic operation using nitrogen as the test gas. This tunnel was used for a variety of tests during the spring and summer of 1972.[3] Based on the experience and confidence gained with the low-speed cryogenic tunnel, a larger pressurized transonic tunnel especially designed for cryogenic operation was built and put into operation during 1973.[8] This tunnel, now known as the 0.3-m Transonic Cryogenic Tunnel (TCT), has been used since August of 1973 to develop cryogenic instrumentation and testing techniques, determine possible operating limits set by condensation or other real-gas effects, study various tunnel control schemes, and gain experience in the operation of a cryogenic nitrogen-gas wind tunnel. In addition, it has been used for a variety of aerodynamic tests that could take advantage of either the high unit Reynolds number or the extremely wide range of Reynolds number available.[9,10] The papers by Ferris[11], Ray[12] and Balakrishna[13] report on some of the results obtained from the 0.3-m TCT in over 2000 hours of operation since 1973. These papers include the experimental work on strain-gage balances, studies related to the tunnel control systems, and experience gained in a variety of areas in the day to day operation of the tunnel.

Based on extensive theoretical studies and the supporting experimental work in the 0.3-m TCT, it was decided to build at the NASA Langley Research Center a large transonic cryogenic tunnel to be known as the National Transonic Facility (NTF). This new tunnel, which is now under construction, will take full advantage of the cryogenic wind tunnel concept to provide an order of magnitude increase in Reynolds number capability over existing tunnels in the United States.

This paper has a twofold purpose. The first is to review the results of some of the real-gas studies made at Langley that are directly related to establishing the range of operating conditions that can be used in a cryogenic nitrogen wind tunnel and still be assured of valid full-scale simulation. Included are theoretical studies to determine if there are any changes in either laminar or turbulent boundary layer characteristics caused by real-gas effects and theoretical and experimental studies to determine the onset of condensation effects in order to establish the effective minimum operating temperature boundaries. The second purpose of this paper is to describe the important aerodynamic features, anticipated performance capability, status of construction, and projected operating date for the NTF.

REAL-GAS STUDIES

For all practical purposes the behavior of the atmosphere under the conditions of temperature and pressure encountered in subsonic and transonic flight is that of an ideal diatomic gas. Thus, in general, the working fluid selected for a wind tunnel must also behave like an ideal diatomic gas. In the cryogenic wind tunnel concept developed at Langley, the working fluid is gaseous nitrogen. At ambient temperature and pressure there is essentially no difference in the behavior of air or nitrogen and an ideal diatomic gas. At cryogenic temperatures, however, both air and nitrogen depart from ideal-gas behavior. The most obvious departure from ideal behavior is the existence of a "saturation boundary" in the p-T plane beyond which a real gas can condense and become a liquid. In addition to having a saturation boundary, both air and nitrogen depart from ideal-gas behavior due to thermal imperfections ($pv \neq RT$) and caloric imperfections (specific heats not constant). Because of these departures from ideal-gas behavior, theoretical and experimental studies have been made to evaluate cryogenic nitrogen as a transonic wind-tunnel test gas.

Boundary Layers. The main purpose of the new high Reynolds number transonic tunnels is to obtain the proper simulation of viscous flow effects in the subsonic and transonic flight regime. The real-gas analysis of cryogenic nitrogen as a transonic wind tunnel test gas previously reported[14] indicates that there

are no significant real-gas effects in simple inviscid flows. The real-gas analysis has therefore been extended to include a study of both laminar and turbulent boundary layers to determine to what extent the imperfection of cryogenic nitrogen might affect these flows and to determine if such effects might impose a more restrictive lower temperature limit for the proper simulation of viscous flows in cryogenic nitrogen wind tunnels.

The prime calculation tool for the boundary-layer study was a program by Anderson and Lewis[15] which solves both the laminar and turbulent compressible boundary-layer equations for either ideal or real gases and is capable of handling two-dimensional and axisymmetric configurations with pressure gradients. The thermodynamic properties of nitrogen based on Jacobsen[16] were interfaced with the program by the use of tables. As a check on the results from the Anderson and Lewis program, a second program based on the similar solution procedure of Cohen[17] for laminar boundary layers was used. For the second program, nitrogen property tables based on the Beattie-Bridgeman equation of state were used.

For analysis purposes, a free-stream Mach number of 0.85 was chosen. A stagnation pressure of 9atm and a stagnation temperature of 120K were used in the analysis because any real-gas effects should be maximized under these extreme operating conditions which lie near the nitrogen saturation boundary and approximate the maximum Reynolds number conditions of the NTF.

Laminar boundary layer; flat plate. The real-gas effects on the laminar boundary layer on a flat plate with zero pressure gradient were studied first because both programs described above were adequate for the analysis. For the assumed test conditions the free-stream Reynolds number is 460 million per meter and one would expect laminar flow only very near the leading edge of the plate. The magnitude of any real-gas effects calculated by the programs will be independent of the value chosen for x, the distance from the leading edge. The boundary-layer characteristics at x = 0.3cm have therefore been chosen to illustrate the results in the laminar-flow region. At 0.3cm, R_x is 1.4 million.

Figure 1 is illustrative of the laminar boundary layer results for both nitrogen and an ideal gas for various wall to total temperature ratios. The local skin-friction coefficients for nitrogen as predicted by the two programs are in excellent agreement, with the coefficient for nitrogen always slightly less than the ideal-gas value. Although not shown, the agreement between the two programs for the other boundary-layer parameters, θ, δ^*, and δ, is just as good.

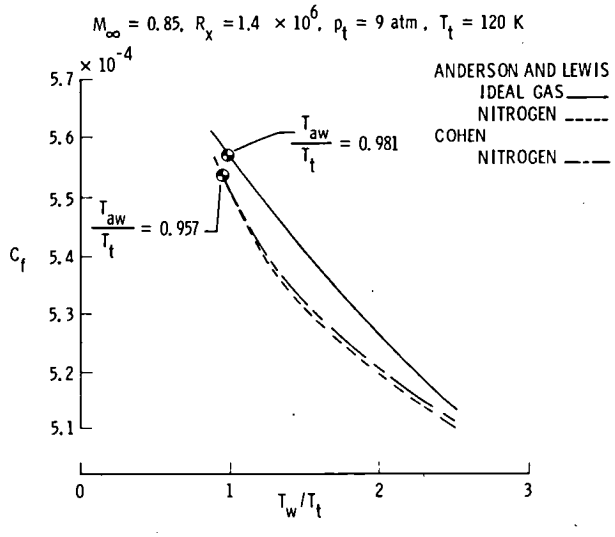

Fig. 1.- Real-gas effects on laminar skin friction for flat plate.

The deviations of the various parameters from the ideal-gas values at the adiabatic wall conditions are given in Table I. None of the deviations are significant except for the deviation of the adiabatic wall temperature itself. As long as the other boundary-layer parameters do not differ significantly from their corresponding ideal-gas values, there seems to be no reason for concern over the fact that the adiabatic wall to stagnation temperature ratio, T_{aw}/T_t, differs from the ideal or flight ratio.

The agreement in the laminar flat plate results obtained from the two programs gives the desired confidence that both programs are working properly and that the thermodynamic properties of nitrogen have been properly interfaced with the programs. Thus, the Anderson and Lewis program was used to analyze the real-gas effects on the turbulent boundary layer on a flat plate.

TABLE I. - DEVIATIONS OF LAMINAR BOUNDARY-LAYER PARAMETERS ADIABATIC FLAT PLATE, R_x = 1.4 MILLION

PARAMETER	NITROGEN VALUE / IDEAL VALUE
C_f	0.992
θ	.993
δ^*	1.000
δ	.999
$\frac{T_{aw}}{T_t}$	.975

Turbulent boundary layer; flat plate. The real-gas effects on the turbulent boundary layer on a flat plate with zero pressure gradient were studied at a distance of 30cm from the leading edge which gives a value of R_x of 140 million, well within the range of Reynolds numbers where turbulent flow would be expected.

Figure 2 shows the boundary-layer parameters C_f, θ, and δ^* as functions of the wall to stagnation temperature ratio, T_w/T_t. At adiabatic conditions the nitrogen values agree well with ideal-gas values, but significant differences are apparent, especially in δ^*, at the higher temperature ratios. It was noted that these differences practically disappear if the results are correlated with the enthalpy ratio, h_w/h_t, as shown in Figure 3, rather than the temperature ratio. For the ideal gas or flight case the temperature and enthalpy ratios are equal. However, for cryogenic nitrogen they are not equal due to the real-gas imperfections ($h \neq c_p T$). The laminar non-adiabatic results also correlate well when the enthalpy ratio, rather than the temperature ratio, is used as the correlation parameter. Thus, in order to simulate non-adiabatic turbulent or laminar boundary layers in a cryogenic nitrogen wind tunnel, the flight enthalpy ratio, rather than the temperature ratio, should be reproduced.

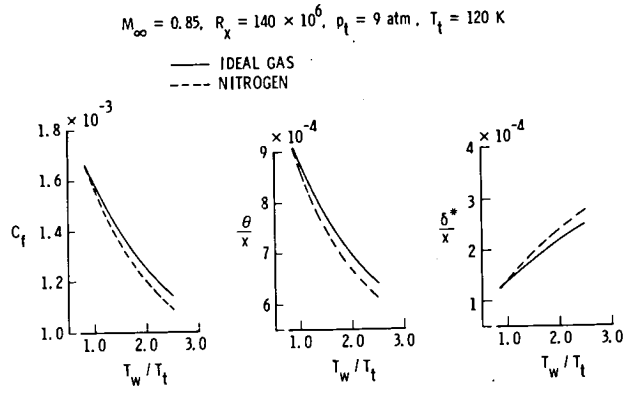

Fig. 2.- Turbulent boundary-layer parameters for flat plate as a function of temperature ratio.

The deviations of the turbulent boundary-layer parameters for nitrogen from those of an ideal gas at the adiabatic wall condition are given in Table II. As was the case for the laminar boundary-layer parameters, none of the deviations are significant except for the adiabatic wall temperature. For these stagnation conditions (9atm, 120K), the 3.3 percent deviation represents a temperature difference of about 4K. Temperature differences of this magnitude should be measurable and such an experiment is planned for the 0.3-m TCT. In these tests, adiabatic wall temperatures will be measured at both cryogenic and ambient

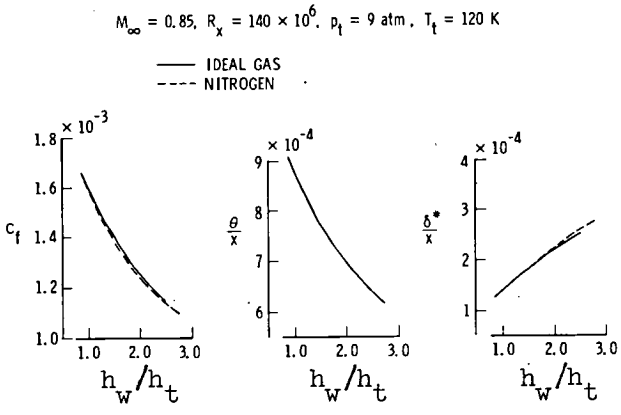

Fig. 3.- Turbulent boundary-layer parameters for flat plate as a function of enthalpy ratio.

temperatures and the resulting temperature ratios, T_{aw}/T_t, compared. These tests should provide experimental verification of the real-gas analytical prediction techniques.

To this point, it has been noted that skin friction and the other integrated boundary-layer properties for cryogenic nitrogen do not differ significantly from those for an ideal gas. The adiabatic turbulent boundary-layer profiles for nitrogen are shown in Figure 4 relative to the ideal-gas profiles.

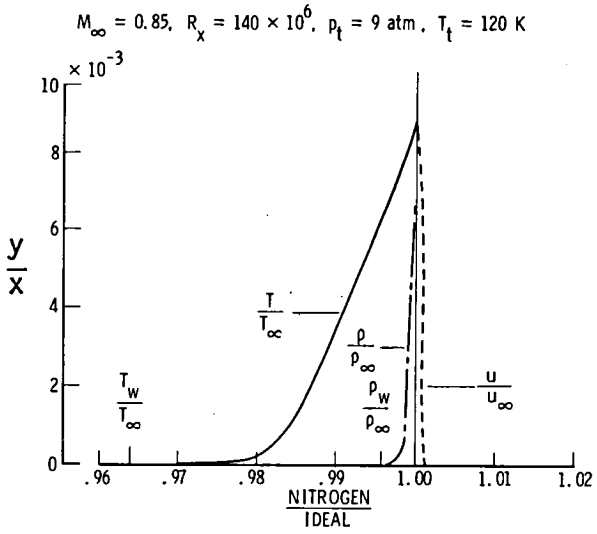

Fig. 4.- Adiabatic turbulent boundary-layer profiles for flat plate, comparison of nitrogen to ideal gas.

TABLE II. - DEVIATIONS OF TURBULENT BOUNDARY-LAYER PARAMETERS ADIABATIC FLAT PLATE, R_x = 140 MILLION

PARAMETER	NITROGEN VALUE / IDEAL VALUE
C_f	0.996
θ	.996
δ^*	1.001
δ	.999
$\frac{T_{aw}}{T_t}$	.967

Note that the density and velocity profiles, which enter directly in the integration for θ and δ^* and in the determination of δ, are not significantly different from the ideal-gas profiles. However, the temperature profile is considerably different. As can be seen, the lower wall temperatures that were noted earlier cause lower temperatures to persist throughout the boundary layer. For real gases such as nitrogen, the boundary-layer equations are solved in terms of enthalpy and velocity rather than in terms of temperature and velocity because real-gas enthalpy is not directly related to temperature ($h \neq c_p T$). For this reason, enthalpy rather than temperature should be considered, as evidenced by the fact that the results correlate well with enthalpy ratio (Fig. 3). Thus, there does not appear to be any significant effect of the cryogenic nitrogen temperature profiles being different from those of an ideal gas.

Turbulent boundary layer; airfoil. The program of Anderson and Lewis was also used to calculate the turbulent boundary layer parameters for a 2-D NACA 0012-64 airfoil at a chord Reynolds number of 140 million. The pressure distribution for zero incidence, sketched as an insert on Figure 5, was input into the program. The Anderson and Lewis program has no provision for shock-boundary layer interaction but can negotiate the adverse pressure gradient caused by the shock. The adiabatic turbulent boundary layer parameters for nitrogen are shown in Figure 5 relative to the ideal-gas values. Nowhere along the chord of the airfoil are the deviations significant except near the leading edge where the numerics of the program begin to affect the deviations.

The results of this boundary-layer analysis indicate that the deviation of the various nitrogen boundary-layer parameters from their ideal-gas values are sufficiently small so as not to impose a lower limit on the tunnel operating temperatures before reaching the saturation boundary. As would be expected, for the less extreme stagnation pressures that would ordinarily be used the deviations of the nitrogen boundary layer parameters are even smaller than those discussed herein. As noted above, previous studies of cryogenic nitrogen have indicated insignificant real-gas effects on inviscid flows. Thus, if there are

no significant real-gas effects on viscous flows as well, as indicated by the present study, it is not likely that there will be large real-gas effects on the cryogenic tunnel simulation of shock boundary-layer interactions or other complex flow conditions encountered in flight.

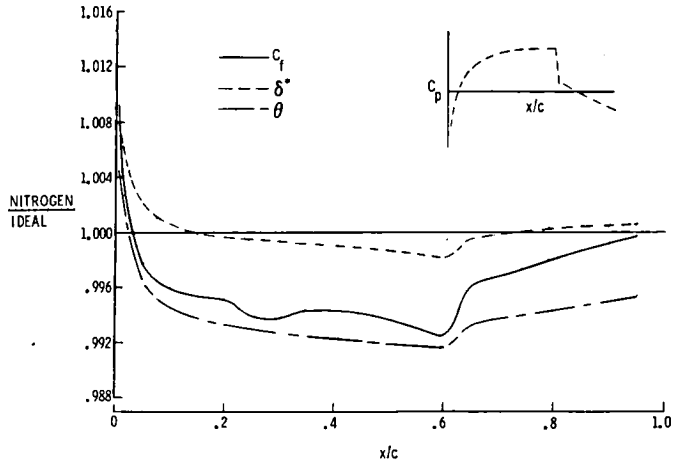

Figure 5.- Adiabatic turbulent boundary-layer parameters for 2-D airfoil. [Nitrogen values related to ideal values. $M_\infty = 0.85$, $R_c = 139 \times 10^6$, $P_t = 9$ atm $T_t = 120$ K]

Minimum Operating Temperatures. A major portion of the real-gas studies has been concerned with determining the minimum usable stagnation temperature. The phrase "minimum usable", in this case, means as low as possible without getting bad data. The main reason for operating at very low temperatures can be seen in Figure 6 which shows the effect of temperature reduction on the properties of nitrogen, the test conditions, and the drive power at a free-stream Mach number of 1 for constant stagnation pressure. The rate of change of Reynolds number with temperature approaches 2 percent per degree Kelvin at the lower temperatures. When testing at cryogenic temperatures, therefore, it is highly desirable to take maximum advantage of reduced temperatures in order to maximize the benefits of cryogenic operation—either increased Reynolds number for a given stagnation pressure or reduced stagnation pressure, and consequently reduced model loads, for a given test Reynolds number. An additional reason to operate at the minimum usable temperature is the reduction in fan-drive power and the corresponding reduction in the amount of liquid nitrogen needed for cooling.

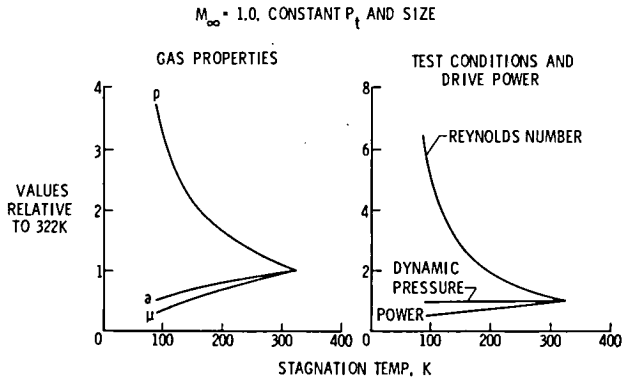

Fig. 6.- Effect of temperature reduction on the gas properties, test conditions, and drive power.

As noted in the previous section, theoretical studies have been made which show the thermal and caloric imperfections of nitrogen at cryogenic temperatures to have no significant effects on either inviscid or viscous flows. The lower temperature boundary for cryogenic tunnel operation is therefore set by the onset of condensation effects.

A conservative approach for selecting the minimum stagnation temperature is to operate at a temperature which avoids any possibility of saturation occurring anywhere over the model. Since the lowest static temperature over a model occurs at the point of maximum local Mach number, a value of T_t can be chosen based on p_t and either the known or anticipated value of the maximum local Mach number in order to keep the local static value of T on the vapor phase side of the saturation boundary. However, such an approach seems to be overly conservative based on experience with airfoils in the 0.3-m TCT and other facilities where condensation effects occur at temperatures lower than those based on maximum local Mach number.

While many studies not directly related to transonic cryogenic tunnels discuss the onset of condensation in nitrogen,[18-21] none cover the relatively high range of static pressures of current interest. Consequently, a theoretical and

experimental program has been underway at Langley to study the onset of condensation of nitrogen at high static pressures in general and to study, in particular, the practical problems caused by condensation in transonic cryogenic nitrogen-gas wind tunnels.

The 0.3-m TCT has been used for two separate experiments in support of these condensation studies. In the first experiment, a 0.137m chord NACA 0012-64 airfoil fitted with static pressure taps was mounted in the test section and the effects of condensation on the static pressure measurements were determined.[22] In the second experiment, four total pressure probes were mounted along the length of the otherwise empty test section and the effects of condensation on the total pressure measurements were determined.

In both of these experiments, the condensation effects are the result of heterogeneous nucleation, that is, droplet growth occurs on "seed" droplets already present in the stream. These seed droplets are the result of incomplete evaporation of the liquid nitrogen injected into the tunnel for cooling. The first evidence that heterogeneous nucleation is occuring can be seen in the airfoil test results. The amount of supercooling that takes place before the onset of condensation for the different free-stream Mach numbers is nearly uniform when the amount of supercooling is calculated based on the free-stream Mach number, rather than maximum local Mach number. The amount of supercooling calculated by the two methods is shown in Figures 7 and 8. Further evidence that heterogeneous nucleation is occurring on seed droplets is seen in Figure 9 which compares the free-stream supercooling from the airfoil tests with the free-stream supercooling realized in the total pressure probe tests. This comparison demonstrates that effects observed in both tests are related to the free-stream conditions since the airfoil was not in the test section during the total pressure probe tests.

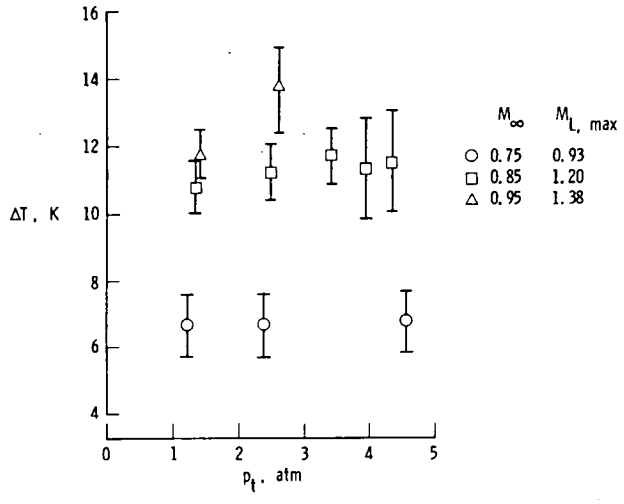

Fig. 7.- Supercooling for airfoil relative to maximum local Mach number.

As can be seen from the data presented in Figures 8 and 9, the onset of condensation effects occurs just slightly below the free-stream saturation temperature. This same situation of heterogeneous nucleation occuring just below free-stream saturation temperature has been seen for the three tests conducted to detect condensation effects in the 0.3-M TCT up to this time; however, the possibility should not be ruled out that homogenous nucleation might occur over an airfoil having a very high local Mach number where there is sufficient supercooling for the gas to condense even in the absence of seed droplets in the free-stream flow.

An idea of the amount of supercooling possible before the onset of homogeneous condensation effects has been given by Sivier.[23] A curve fitted to Sivier's predicted onset conditions is shown in Figure 10 along with the static values of p and T based on the maximum local Mach number present at the onset of condensation effects for the airfoil test in the 0.3-m TCT. Indeed, the onset of condensation effects seen during the airfoil test occur before Sivier's predicted conditions for onset, as would be expected for the case of onset resulting from the presence of seed particles. Nevertheless, the curve fitted to Sivier's predicted conditions for the onset of condensation resulting from homogeneous nucleation appears reasonable and can be used as a rough guide to

determine when one might expect to see such homogeneous effects in a cryogenic tunnel. For example, if an airfoil were to have a maximum local Mach number 1.7 when tested at a free-stream Mach number of 0.9, the conditions at which the onset of condensation effects might occur due to homogeneous nucleation are shown in Figure 11 by the dashed curve developed from Sivier's prediction. Curves corresponding to the pertinent saturation conditions are also shown. For this example, significant supercooling beyond the maximum local Mach number boundary is predicted. However, if homogeneous nucleation does occur as a result of the high local Mach

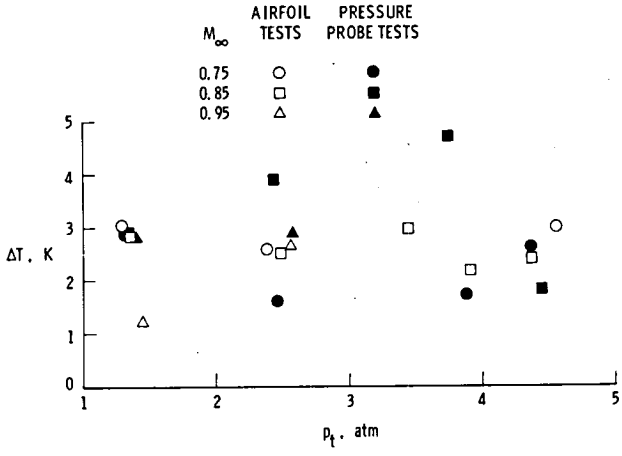

Fig. 9.- Supercooling for airfoil and total pressure probe relative to free-stream Mach number.

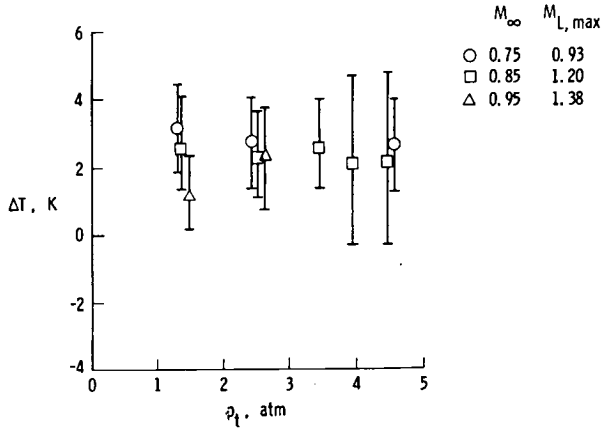

Fig. 8.- Supercooling for airfoil relative to free-stream Mach number.

number, the onset of condensation effects might be seen at a temperature higher than free-stream saturation temperature.

The investigation of minimum operating temperatures is continuing and is now focusing on the relationship between the liquid nitrogen injection process and condensation onset in the test section. In particular, work is now in progress to develop a numerical model to approximate the formation of the liquid droplets and their passage around the tunnel circuit. Additional work is planned with the aim of understanding the interaction between the droplets and the turbulence damping screens, and the role, if any, played by impurities in the liquid nitrogen.

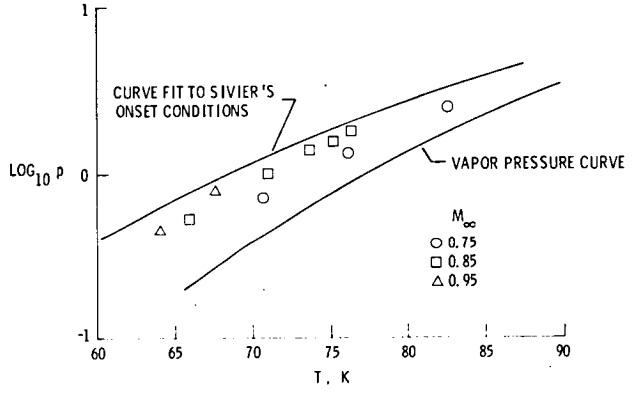

Fig. 10.- Comparison of airfoil supercooling with predicted onset conditions for homogeneous nucleation. p in atmospheres.

THE U.S. NATIONAL TRANSONIC FACILITY

As mentioned in the introduction, the application of the cryogenic wind tunnel concept for high Reynolds number transonic test capability in the United States has culminated in a wind tunnel project known as the National Transonic Facility (NTF). The rationale behind the selection of the performance, size, and pressurization for the NTF has been discussed previously

by McKinney and Howell[24,25] and by Nicks[26]. In essence, the objective has been to achieve full-scale Reynolds numbers for the cruise or other design point, and to match as much of the performance envelope as possible for current and future commercial and military aircraft. The sizing criteria obtained in this way, combined with the constraints imposed by dynamic pressure and cost, resulted in the performance and dimensional characteristics shown in Table III. References 24-27 present excellent descriptions of the NTF as its characteristics evolved during the design process. What follows is essentially a review and update of these previous publications.

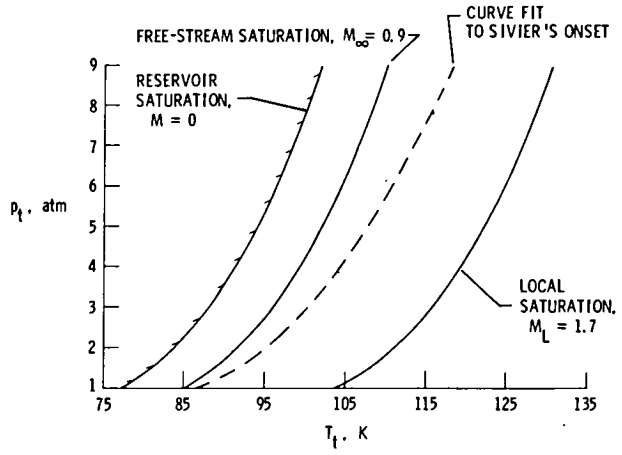

Fig. 11.- Predicted onset of homogeneous nucleation.

TABLE III. - NTF PERFORMANCE CHARACTERISTICS

MACH NUMBER RANGE	0.1 TO 1.2	
REYNOLDS NUMBER RANGE	3×10^6 TO 120×10^6 AT M = 1.0 FOR $\bar{c}$ = .25 m	
PRESSURE RANGE	1 TO 8.85 ATM	
TEMPERATURE RANGE	78K TO 339K	
TEST GAS	NITROGEN, AIR	
TEST SECTION SIZE	2.5 m SQUARE	
LENGTH	7.62 m	
AREA	6.203 m^2	
CONTRACTION AREA RATIO	14.95 TO 1	
CIRCUIT LENGTH	151.5 m	
VOLUME	6600 m^3	
DRIVE POWER,	10 MINUTES	CONTINUOUS
INDUCTION MOTORS	49.2 MW	35.1 MW
SYNCHRONOUS MOTOR	44.8 MW	31.3 MW
TOTAL	94.0 MW	66.4 MW

Current Configuration. The NTF is, in most respects, a rather conventional wind tunnel with only a few unconventional features. These features, some of which may be seen in Figures 12 and 13, are those primarily associated with the cryogenic mode of operation. A few examples of such features are liquid nitrogen injection nozzles, a gaseous nitrogen exhaust vent stack, internal thermal insulation, test section isolation valves, and of course, the materials of construction. The principal materials of construction have been various aluminum alloys, 300 series stainless steels, 9 percent nickel steel, and fiberglass reinforced plastics. None of the unconventional features have imposed any serious gas-dynamics or fluid-mechanics problems, although many of them represent challenging engineering design problems.

As shown in Figure 14, the NTF is a closed circuit wind tunnel with a conventional fan drive capable of continuous operation. At cryogenic temperatures, nitrogen is used as the test gas with cooling accomplished by injecting liquid nitrogen directly into the tunnel circuit upstream of the fan nacelle. At ambient temperature, either air or nitrogen can be used as the test gas with cooling accomplished by a conventional chilled-water heat exchanger inside the tunnel circuit downstream of the rapid diffuser. The need to restrict the capital cost of the pressure shell as well as the operating cost associated with pressurizing the tunnel led to a relatively compact circuit design as shown in the plan view sketch of Figure 14.

As mentioned earlier, the thermal insulation for the tunnel is inside rather than outside the pressure shell. Because of the internal insulation, the pressure shell with its large thermal inertia is not directly involved in changes in gas temperature, thus reducing liquid nitrogen requirements, and also avoiding thermal cycling of the pressure shell which enhances its service life. The insulation is entirely shielded from the flow stream by a flow liner through the high speed portion of the tunnel from corner number 4 to corner number 1. In

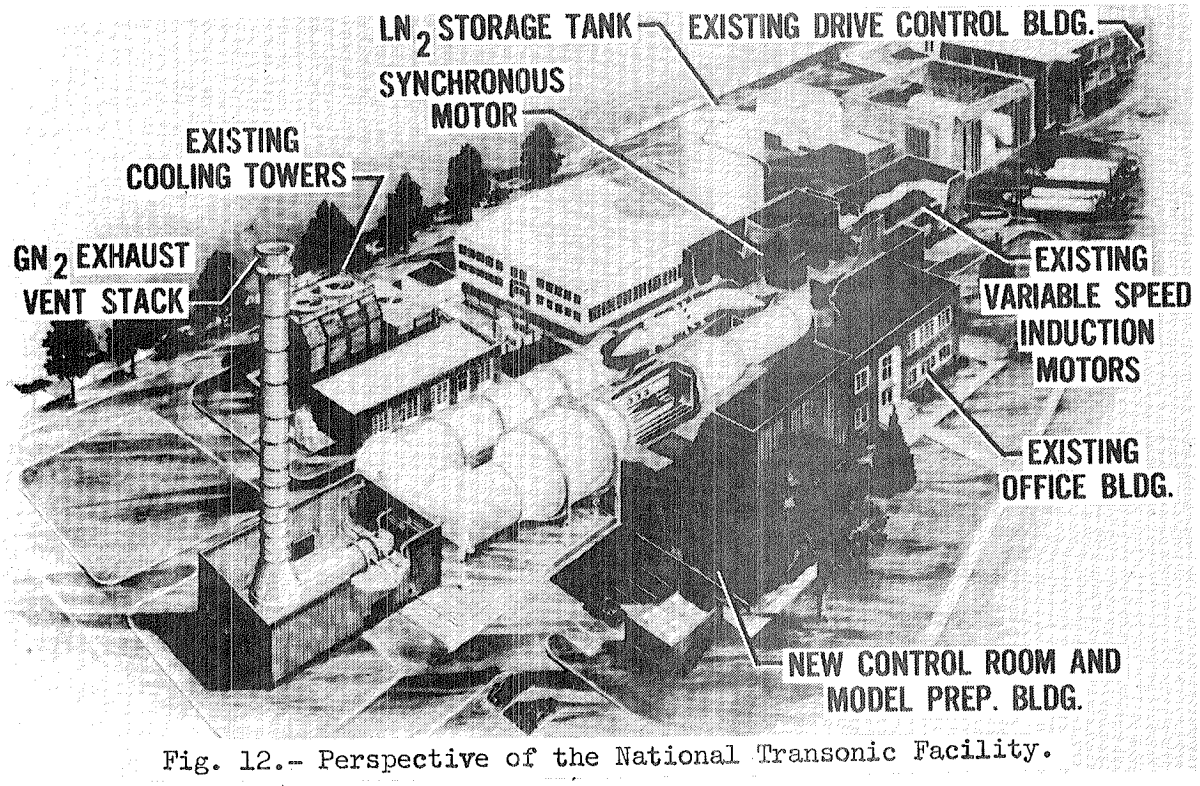

Fig. 12.- Perspective of the National Transonic Facility.

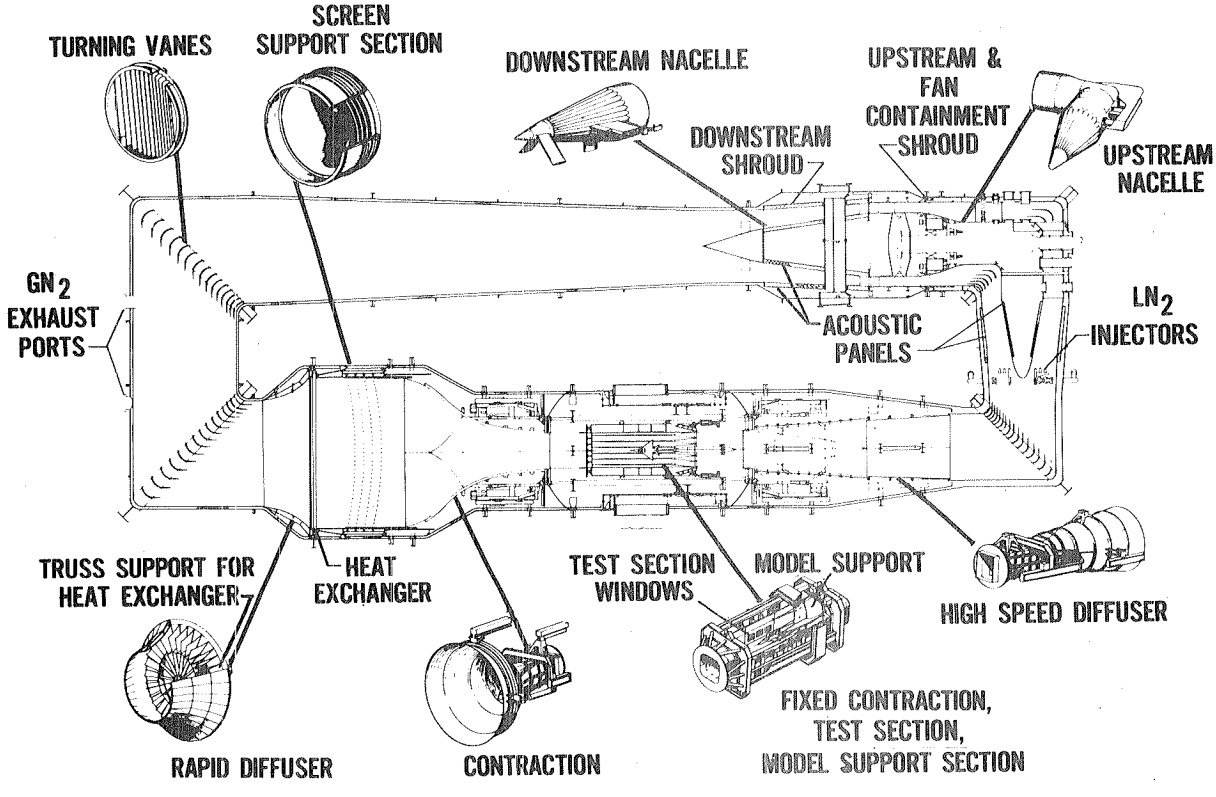

Fig. 13.- Planview of the NTF circuit showing internal structures.

the remainder of the tunnel circuit except for the fan shroud region, the insulation is separated from the flow stream by a thin metal liner. For economy of fabrication, the liner plates are flat, leading to a polygonal cross-section in those parts of the tunnel where these plates are installed.

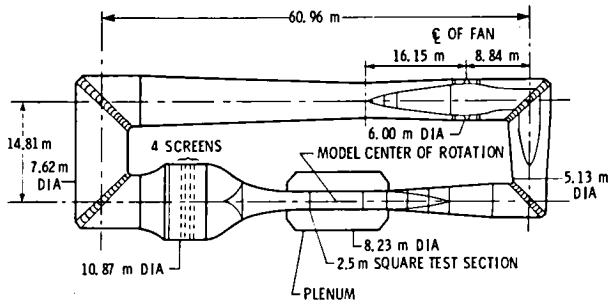

Fig. 14.- Circuit lines of the NTF.

The use of a rapid diffuser upstream of the settling chamber allowed the return duct of the tunnel circuit to be relatively small in diameter but still permitted a large settling chamber. The rapid diffuser itself has an exit to inlet area ratio of about 2, a length to inlet diameter ratio slightly less than 0.5, and an exit wall angle of about 60 degrees. A downstream pressure loss on the order of 3q to 5q is required to prevent flow separation from the walls of the rapid diffuser. This pressure loss will be provided by the chilled-water heat exchanger.

Downstream of the heat exchanger, the settling chamber contains four anti-turbulence screens spaced about 0.61m apart. Each screen has a wire diameter of about 0.81mm and a square mesh wire spacing of about 0.42cm with a resulting solidity ratio of about 0.35. The overall pressure loss through the four screens is about 3q.

The settling chamber is followed by a 14.95 to 1 area ratio contraction. There is an early transition from round to square cross-section with circular arc corner fillets. About 2.8m ahead of the test section the corner fillets are flattened and are continued flat through the test section.

The test section, as shown in Figure 15 is 7.62m long and 2.5m square with flat corner fillets resulting in a cross-sectional area of 6.203m^2. The test section wall ventilation consists of longitudinal slots, 6 in each of the top and bottom walls and 2 in each of the side walls. The side walls are parallel, with provision for 3 large windows and several smaller ports for lighting and viewing. The top and bottom walls are hinged with flexure plates at their upstream end to permit variable wall divergence, and also have lighting and viewing ports in them. The reentry flaps in the slots are remotely adjustable over an angle range of about 15 degrees.

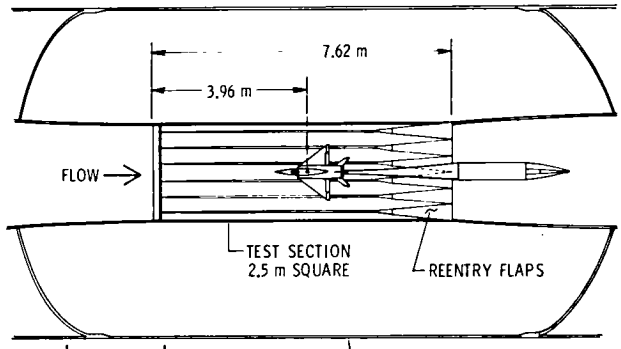

	ANGLE RANGE	MAX RATE
PITCH	-11° TO 19°	4°/sec
ROLL	± 180°	10°/sec

Fig. 15.- Plan view of the NTF slotted test section and plenum.

Generally, test models will be sting supported from a circular arc strut permitting a pitch range of 30 degrees. The pitch angle can be varied at rates up to 4 degrees per second and will be capable of both pitch-pause and continuous sweep operation. The model roll angle range is ± 180 degrees at roll rates up to 10 degrees per second. Sideslip angles are obtained from combinations of pitch and roll. These and other operational characteristics of the NTF are summarized in Table IV.

The sidewalls adjacent to the model support strut are indented to relieve strut blockage. The top and bottom walls in the model support region are hinged with flexure plates at the downstream end so that their divergence angle can be

varied. For strut pitch angles greater than 11 degrees, doors in the bottom wall are provided to permit the strut centerbody to pass below the level of the bottom wall.

The test section and model support section are surrounded by a plenum 8.23m in diameter. Test section isolation valves are located at the upstream and downstream ends of the plenum. In order to deploy the isolation valves, the contraction and the high speed diffuser are retracted upstream and downstream respectively. With the isolation valves in the closed position the plenum and test section can be brought to atmospheric pressure. In this condition the plenum and test section access doors can be opened, and access tunnels can be inserted from both sides providing direct access to the model at ambient temperature and pressure conditions. Access time to the model is estimated to be about 30 minutes.

TABLE IV. - NTF OPERATIONAL CHARACTERISTICS

MAXIMUM MODEL LOADS,	NORMAL	86.7 kN (19,500 LB)
	AXIAL	41.4 kN (9,356 LB)
	SIDE	44.5 kN (10,000 LB)
PITCH ANGLE RANGE		-11 DEG TO 19 DEG
RATE		UP TO 4 DEG/SEC
ROLL ANGLE RANGE		±180 DEG
RATE		UP TO 10 DEG/SEC
ACCESS TIME TO MODEL		30 MIN
COOLDOWN/WARMUP TIME, $\Delta T = 222K$		5 HR COMPLETE TUNNEL
$\Delta T = 39K$		NO TIME LIMIT
MODEL DATA		448 ANALOG CHANNELS
	PRESSURE PORTS	276 (MECHANICAL SCANNER)
	OR	1024 (ELECTRONIC SCANNER)
	FORCE	3 S.G. BALANCES (6 COMPONENTS)
	ACCELEROMETERS	3
	THERMOCOUPLES	12

The high speed diffuser begins at the downstream end of the model support section with a transition from rectangular to round cross-section in about the first 9m of its length. Overall, the high speed diffuser has an area expansion equivalent to a conical diffuser with about a 2.6 degree half angle.

The turning vanes in all four corners have what is known as arithmetic progression spacing, introduced by Dimmock[28] for gas turbine work, and used successfully in other wind tunnels.

The upstream fan nacelle fairing is bent through corner number 2, with the fan located 8.84m downstream of that corner. The single-stage fan has 25 fixed-pitch blades with fan loading changed by 24 variable inlet guide vanes (IGV) and by variable rotational speed. There are 26 fixed downstream stators.

As indicated in Figure 13, acoustic panels are located in the fan nacelle and the adjacent tunnel walls at the nose and tail cone of the nacelle. These panels are intended to attenuate fan noise propagating upstream and downstream from the fan station and provide about a 13db reduction of fan noise reaching the test section.

As mentioned earlier, the liquid nitrogen injection nozzles are located upstream of the fan nacelle as indicated in Figure 13. It has been shown[29] that liquid nitrogen injection upstream of the fan results in lower power requirements and liquid nitrogen flow-rates compared to downstream injection. An added benefit of this location may be a reduction of injection noise levels reaching the test section.

The NTF fan will be powered by two variable speed induction motors (49.2MW) and a synchronous motor (44.8MW). As shown in the upper part of Figure 16, the induction motors are coupled to the fan drive shaft through a two-speed gear box with gear ratios (motor to fan speed) of 835/360 in low gear and 835/600 in high gear. The purpose of the two-speed gear box is to provide a better match of the motor torque available to the fan torque required at different operating temperatures. The synchronous motor is in line with the fan drive shaft and rotates at fan speed at all times.

The maximum (10 minute rating) shaft power available from the drive motor combination as a function of fan rotational speed is shown in the lower part of Figure 16, for both the high and low gear ratios. The synchronous motor is operated at the fan shaft speed corresponding to the maximum speed of the induction motors in the low gear ratio, and is brought up to synchronous speed by the induction motors.

Performance. To determine the NTF performance capabilities, the power characteristics of Figure 16 must be combined with the tunnel pressure ratio requirements and the fan design characteristics. These NTF characteristics have been combined by Gloss of LRC to obtain operating envelope curves such as the one shown in Figure 17 for a free-stream Mach number of 1.0. The envelopes are in the form of stagnation pressure versus Reynolds number with lines of constant temperature superimposed. The maximum operating envelope is shown by the hatched line, with boundaries formed on the left by maximum operating temperature or inlet guide

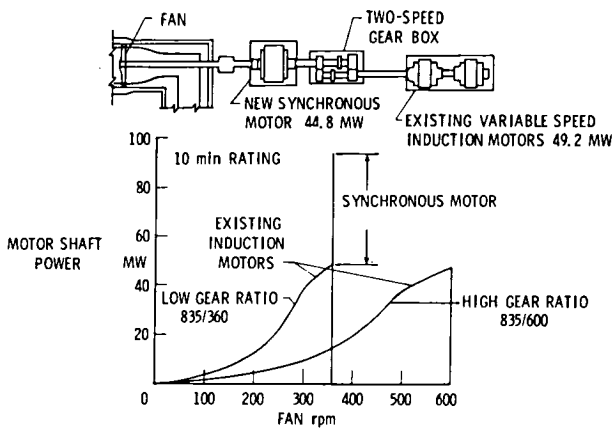

Fig. 16.- NTF drive system power.

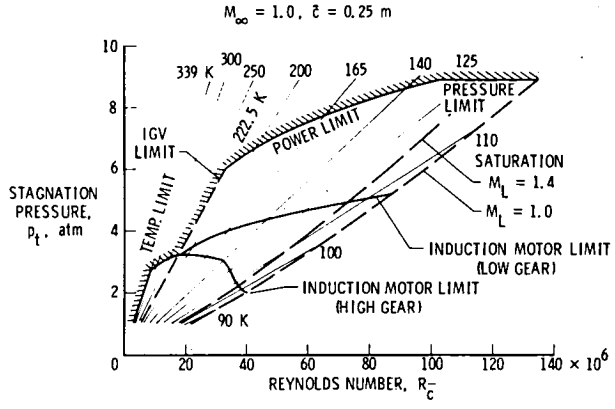

Fig. 17.- NTF operating envelope of stagnation pressure and Reynolds number for a Mach number of 1.0.

vane limits, across the top by power or shell pressure limits, and on the right by permissable saturation levels. Two saturation lines are shown, one for saturation conditions corresponding to a local Mach number of 1.4; the other for saturation at free-stream conditions. The lower power boundaries are for the induction motors alone in the low gear or high gear settings.

In general, the maximum Reynolds number occurs where the permissable saturation lines intersect either the shell pressure limit line (as is the case for Mach numbers from 0.1 to slightly above 1.0) or the maximum power limit (as is the case for higher Mach numbers). An envelope of maximum Reynolds number for the NTF is shown as a function of Mach number in Figure 18 for two saturation boundaries. The upper boundary is for saturation at free-stream conditions. The condensation studies described earlier have indicated that the onset of condensation effects may not be apparent until free-stream saturation conditions are reached or even exceeded. A slightly more conservative boundary corresponding to saturation conditions at a local Mach number 0.4 above the free-stream Mach number is also shown. With a representative chord taken as one tenth of the square root of the test section area, the more conservative saturation boundary is seen to reach a maximum Reynolds number based on chord of about 120 million at a Mach number of 1.0. The less conservative saturation boundary reaches a Reynolds number of about 135 million. At these peak Reynolds numbers, the dynamic pressure is about 3.35atm for either boundary.

As mentioned earlier, the NTF will be capable of operating in an ambient temperature mode using either air or nitrogen as the test gas with cooling accomplished by a conventional chilled-water heat exchanger. The heat exchanger capacity corresponds to a power input of about 35MW. At the lower part of Figure 18, the maximum Reynolds number for the NTF in this mode is shown along with the maximum Reynolds number for existing wind tunnels in the U.S. The advantages of cryogenic operation are quite obvious in comparison.

Construction Status. Most of the major items of construction for the NTF are now under contract. Figure 19, an aerial view of the NTF construction site, shows that the foundation is now completed, and substantial portions of the pressure shell have been set in place. The locations of corners 2, 3, and 4 form an outline of the tunnel circuit. Construction has also started on the liquid nitrogen storage tank. Other elements of the existing structure and equipment are also shown in the photograph.

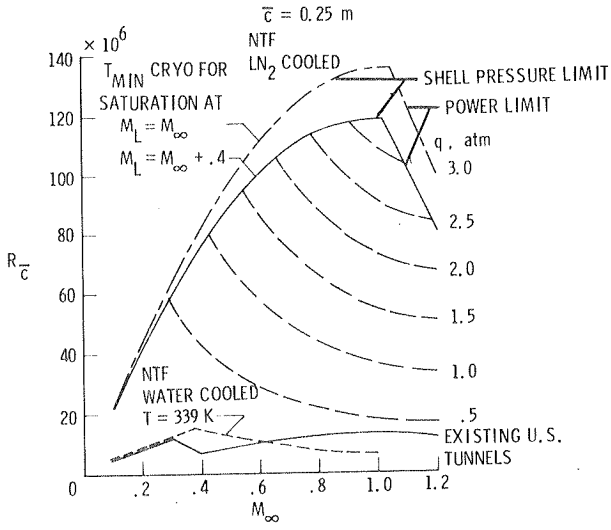

Fig. 18.- Maximum Reynolds number as a function of Mach number for the NTF.

The NTF construction schedule shown in Table V lists some of the completion dates and other major events for the tunnel. The completion of the hydraulic pressure test in mid 1980 is one of the significant milestones since the installation of the internal insulation and final alignment of internal structures cannot begin until after that time. As presently scheduled, initial shakedown operation of the tunnel could take place in late 1981 or early 1982. The completion of the operational readiness review in mid 1982 signals the readiness of the tunnel to be placed into routine operation.

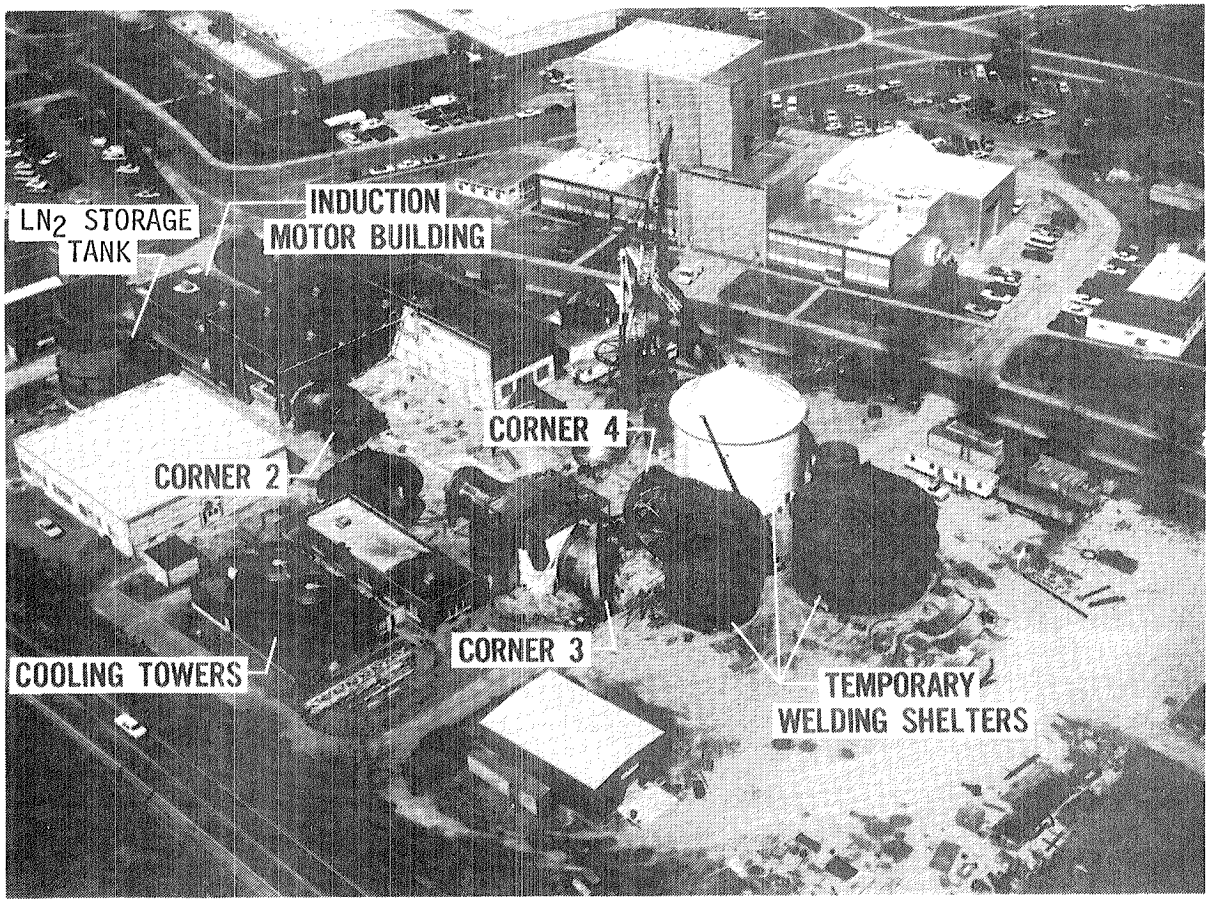

Fig. 19.- Aerial view of the NTF construction site.

CONCLUDING REMARKS

Theoretical studies have been made to determine the effect of thermal and caloric imperfections in cryogenic nitrogen on both laminar and turbulent boundary layers. The results indicate that in order to simulate non-adiabatic laminar or turbulent boundary layers in a cryogenic nitrogen wind tunnel, the flight enthalpy ratio, rather than the temperature ratio, should be reproduced. Under adiabatic conditions the difference between wind tunnel and flight boundary layer parameters is negligible except for the surface temperature ratio. No significance can be attached to the difference in temperature ratio. The absence of significant real-gas effects on both viscous and inviscid flows makes it unlikely that there will be large real-gas effects on the cryogenic tunnel simulation of shock boundary-layer interactions or other complex flow conditions encountered in flight.

TABLE V. - NTF CONSTRUCTION SCHEDULE

ITEM	COMPLETION DATE
FOUNDATION	FEB. 1979
LN_2 STORAGE	OCT. 1979
HYDRO TEST	JULY 1980
PRESSURE SHELL COMPLETED	AUG. 1980
INTERNALS FABRICATION COMPLETED	DEC. 1980
DRIVE SYSTEM	APR. 1981
GN_2 VENT STACK	APR. 1981
FAN BLADE INSTALLATION	MID 1981
INSULATION	NOV. 1981
INTERNALS INSTALLATION COMPLETED	NOV. 1981
DATA ACQUISITION SYSTEM	NOV. 1981
PROCESS CONTROL	NOV. 1981
BUILDING	NOV. 1981
INTEGRATED SYSTEMS REVIEW	NOV. 1981
OPERATIONAL READINESS REVIEW	JULY 1982

Experimental and theoretical studies on condensation effects have been made to determine the minimum usable stagnation temperature. Considerable evidence indicates that under most circumstances free-stream Mach number rather than maximum local Mach number determines the relevent saturation boundary and thereby determines the onset of condensation effects. Under extremely high local Mach number conditions, however, homogeneous nucleation could occur and the onset of condensation effects might be seen at temperatures higher than free-stream saturation temperature but still considerably lower than local Mach number saturation temperature.

Progress is well underway on a major application of the cryogenic wind-tunnel concept with the construction of the U.S. National Transonic Facility at the NASA Langley Research Center. This new tunnel is scheduled to become operational by 1982. Not only will it provide an order of magnitude increase in Reynolds number capability over existing U.S. tunnels, but also, because of the ability to vary pressure, Mach number, and temperature independently, it will be able to perform the highly desirable research task of separating aeroelastic, compressibility, and viscous effects on the aerodynamic parameters being measured.

REFERENCES

1. ANON.: Proceedings of the AGARD Conference on Facilities and Techniques for Aerodynamic Testing at Transonic Speeds and High Reynolds Number, Göttingen, Germany, Aug. 1971. AGARD CP No. 83.

2. ANON.: Proceedings of the AGARD Conference on Wind Tunnel Design and Testing Techniques, London, U.K., Oct. 1975. AGARD CP No. 174.

3. Kilgore, Robert A.; Goodyer, Michael J.; Adcock, Jerry B.; and Davenport, Edwin E.: The Cryogenic Wind-Tunnel Concept for High Reynolds Number Testing. NASA TN D-7762, 1974.

4. Margoulis, W.: Nouvelle méthode d'essai de modèles en souffleries aérodynamiques. Compts Rendus Acad. Sci. Vol. 171, 1920, pp 997-999 (Séance du 22 November 1920).

5. Margoulis, W.: A New Method of Testing Models in Wind Tunnels. NACA TN No. 52, August, 1921.

6. Smelt, R.: Power Economy in High-Speed Wind Tunnels by Choice of Working Fluid and Temperature. Rep. No. Aero. 2081, Brit. R.A.E., Aug. 1945.

7. Goodyer, Michael J.; and Kilgore, Robert A.: The High Reynolds Number Cryogenic Wind Tunnel. AIAA Paper No. 72-995, Sept. 1972.

8. Kilgore, Robert A.: Design Features and Operational Characteristics of the Langley Pilot Transonic Cryogenic Tunnel. NASA TM X-72012, 1974.

9. Reubush, D. E., and Putnam, L. E.: An Experimental and Analytical Investigation of the Effect on Isolated Boattail Drag of Varying Reynolds Number up to 130 Million. NASA TN D-8210, May 1976.

10. Reubush, D. E.: Effect of Reynolds Number on the Subsonic Boattail Drag of Several Wing-Body Configurations. NASA TN D-8238, July 1976.

11. Ferris, Alice T.: Cryogenic Wind Tunnel Force Instrumentation. Paper No. 32, First International Symposium on Cryogenic Wind Tunnels, Southampton, England, 3-5 April 1979.

12. Ray, Edward J., et al.: Review of Design and Operational Characteristics of the 0.3-meter Transonic Cryogenic Tunnel. Paper No. 28, First International Symposium on Cryogenic Wind Tunnels. Southampton, England, 3-5 April, 1979.

13. Balakrishna, S.: Modeling and Control of a LN_2 - GN_2 Operated Closed Circuit Cryogenic Wind Tunnel. Paper No. 23, First International Symposium on Cryogenic Wind Tunnels. Southampton, England, 3-5 April, 1979.

14. Adcock, Jerry B.: Real-Gas Effects Associated with One-Dimensional Transonic Flow of Cryogenic Nitrogen. NASA TN D-8274, 1976.

15. Anderson, E. C.; and Lewis, C. H.: Laminar or Turbulent Boundary-Layer Flows of Perfect Gases or Reacting Gas Mixtures in Chemical Equilibrium. NASA CR-1893, 1971.

16. Jacobsen, R. T.; et al.: Thermophysical Properties of Nitrogen From the Fusion Line to 3500R (1944K) for Pressures to 150,000 psia (10,342 x 10^5 N/m^2) NBS Tech. Note 648, U.S. Dep. Com., Dec. 1973.

17. Cohen, Nathaniel B.: Boundary-Layer Similar Solutions and Correlation Equations for Laminar Heat-Transfer Distribution in Equilibrium Air at Velocities Up to 41,000 Feet per Second. NASA TR R-118, 1961.

18. Wegener, P.P.; and Mack, L. M.: Condensation in Supersonic and Hypersonic Wind Tunnels. Advances in Applied Mechanics, Vol. V, 1958, pp. 307-447.

19. Daum, Fred L.; and Gyarmathy, George: Condensation of Air and Nitrogen in Hypersonic Wind Tunnels. AIAA Journal, Vol. 6, No. 3, Mar. 1968, pp. 458-465.

20. Goglia, Gennaro L.; and Van Wylen, Gordon J.: Experimental Determination of Limit of Supersaturation of Nitrogen Vapor Expanding in a Nozzle. Journal of Heat Transfer, Vol. 83, Series C, No. 1, Feb. 1961, pp. 27-32.

21. Dankert, C.; and Koppenwallner, G.: An Experimental Study of Nitrogen Condensation in a Free Jet. Eleventh International Symposium on Rarefied Gas Dynamics, Cannes, July, 1978.

22. Hall, Robert M.: Onset of Condensation Effects with a NACA 0012-64 Airfoil Tested in the Langley 0.3-meter Transonic Cryogenic Tunnel. NASA TP-1385, 1979.

23. Sivier, Kenneth D.: Digital Computer Studies of Condensation in Expanding One-Component Flows. Aerospace Research Laboratories Report ARL 65-234, November, 1965.

24. McKinney, Linwood W.; and Howell, Robert R.: The Characteristics of the Planned National Transonic Facility. Paper presented at the AIAA 9th Aerodynamic Testing Conference, Arlington, Texas, June 7-9, 1976.

25. Howell, Robert R.; and McKinney, Linwood W.: The U. S. 2.5 Meter Cryogenic High Reynolds Number Tunnel. Proceedings of the Workshop on High Reynolds Number Research, Oct. 27-28, 1976, Donald D. Baals, ed. NASA CP-2009, 1977, pp. 27-51 (also paper presented at the 10th Congress of the International Council of the Aeronautical Sciences (ICAS), Ottawa, Canada, Oct. 3-9, 1976).

26. Nicks, Oran W.: The NTF as a National Facility. Proceedings of the Workshop on High Reynolds Number Research, Oct. 27-28, 1976, Donald D. Baals, ed, NASA CP-2009, 1977, pp. 19-25.

27. Nicks, Oran W.; and McKinney, Linwood W.: Status and Operational Characteristics of the National Transonic Facility. Paper presented at the AIAA 10th Aerodynamic Testing Conference, San Diego, California, April 19-21, 1978.

28. Dimmock, N. A.: The Development of a Simply Constructed Cascade Corner for Circular Cross Section Ducts. N.G.T.E.M. 78, Feb. 1950.

29. Adcock, Jerry B.: Effect of LN_2 Injection Station Location of the Drive Fan Power and LN_2 Requirements of a Cryogenic Wind Tunnel. NASA TM X-74036, June, 1977.

1. Report No.	2. Government Accession No.	3. Recipient's Catalog No.
NASA TM 80085		

4. Title and Subtitle	5. Report Date
FULL-SCALE AIRCRAFT SIMULATION WITH CRYOGENIC TUNNELS AND STATUS OF THE NATIONAL TRANSONIC FACILITY	April 1979
	6. Performing Organization Code

7. Author(s)	8. Performing Organization Report No.
Robert A. Kilgore, William B. Igoe, Jerry B. Adcock, Robert M. Hall, and Charles B. Johnson	
	10. Work Unit No. 505-06-43-08

9. Performing Organization Name and Address	11. Contract or Grant No.
Langley Research Center Hampton, VA 23665	
	13. Type of Report and Period Covered
12. Sponsoring Agency Name and Address	Technical Memorandum
National Aeronautics and Space Administration Washington, DC 20546	14. Sponsoring Agency Code

15. Supplementary Notes

Material presented as paper no. 11, First International Symposium on Cryogenic Wind Tunnels, Southampton, England, April 3-5, 1979

16. Abstract

Theoretical studies to determine the effect of thermal and caloric imperfections in cryogenic nitrogen on boundary layers indicate that in order to simulate nonadiabatic laminar or turbulent boundary layers in a cryogenic nitrogen wind tunnel, the flight enthalpy ratio, rather than the temperature ratio, should be reproduced. The absence of significant real-gas effects on both viscous and inviscid flows makes it unlikely that there will be large real-gas effects on the cryogenic tunnel simulation of shock boundary-layer interactions or other complex flow conditions encountered in flight.

Experimental and theoretical studies on condensation effects to determine the minimum usable temperature indicate that under most circumstances free-stream Mach number rather than maximum local Mach number determines the onset of condensation effects. However, if homogeneous nucleation occurs, the onset of condensation effects might be seen at temperatures higher than free-stream saturation temperature but still considerably lower than local Mach number saturation temperature.

Progress is well underway on a major application of the cryogenic wind-tunnel concept with the construction of the U.S. National Transonic Facility at the Langley Research Center. This new tunnel is scheduled to become operational by 1982.

17. Key Words (Suggested by Author(s))	18. Distribution Statement
Boundary layers Condensation Cryogenics Real gases Transonic wind tunnel	Unclassified - Unlimited Star Category - 09

19. Security Classif. (of this report)	20. Security Classif. (of this page)	21. No. of Pages	22. Price*
Unclassified	Unclassified	18	$4.00

*For sale by the National Technical Information Service, Springfield, Virginia 22151

End of Document